

EXPERIMENTAL AND NUMERICAL ANALYSIS CORRELATION OF HAIL ICE IMPACTING COMPOSITE STRUCTURES

Hyonny Kim and Keith T. Kedward*
Department of Mechanical and Environmental Engineering
University of California, Santa Barbara, California

Abstract

Many composite aircraft structures such as fuselage and wing skins, engine nacelles, and fan blades are situated such that hail ice impacts are a realistic threat. To investigate this threat, high velocity impact experiments and subsequent numerical analyses were performed to study hail ice impacts on composite structures. As hail ice is not a well characterized impact material, cast ice spheres made to simulate hail ice were projected onto a force measurement transducer system with the motivation of studying and gaining insight into ice as a projectile. Simulated hail ice was then projected onto thin carbon/epoxy composite fabric panels to study their impact damage resistance. Several of the tests involved impacts onto instrumented panels in which no damage occurred. For these test panels, their dynamic response was measured with the intent of future analytical correlation. This paper presents a numerical simulation of impacts onto a force measurement transducer and an instrumented panel impact test in which no damage occurred. The analyses were correlated with the experimental data and have been found to adequately model the impact behavior of ice and the elastic response of a thin composite panel.

Introduction

Laminated polymer composites have found widespread use in the design of aerospace structures. While these materials offer excellent in-plane performance, they are susceptible to damage when severely loaded out-of-plane, such as in the case of impacts. Often the damage resulting from impacts is barely visible and exists in the form of subsurface matrix cracks, backside fiber failure, and delaminations. The latter two damage forms can significantly degrade a structure's performance. This paper focuses on the transverse impact of flexible composite structures by high velocity hail ice; a realistic threat which exists

both while in-flight and on the ground. Much work previously has focused on the impact of thick composite plates by low velocity metallic impactors¹⁻⁷ which behave elastically during the impact event. Ice as a high velocity projectile on the other hand exhibits significant permanent deformation and crushing⁸ and is a material for which mechanical properties are still currently under investigation^{9,10}.

Since the existence of barely visible impact damage (BVID) can be a significant safety threat, the ability to predict such damage is of great interest. The objective of this paper therefore is to predict the response of a composite panel target to impact by high velocity ice, and to correlate these predictions with experiments¹¹. While this paper is limited to predicting only the elastic response of a panel with no damage occurring, such a prediction is a necessary step before proceeding on to predicting the experimentally observed impact damage modes. In prelude to simulating ice impacts on composite targets, the behavior of ice as an impactor needs to be understood and carefully modeled. Therefore the modeling of ice impacts onto an instrumented target has also been undertaken and is reported herein.

Experiments

To investigate the hail ice impact threat, simulated hail ice (SHI) was projected using a nitrogen gas cannon, shown in Figure 1, located at Pratt & Whitney's East Hartford Applied Mechanics laboratory¹¹. Figure 2 shows the construction of the SHI. The monolithic ice spheres were cast in one filling session, and the flat-wise layered spheres were constructed by casting the ice spheres over ten to eleven filling sessions. The motivation for the layered ice sphere was to produce a projectile which was tougher than a monolithic sphere. Actual hail ice has more of a spherically layered construction composed of many thin layers. The sizes of SHI tested were 1.0, 1.68 (golf ball size), and 2.0 in. diameter.

The cannon projected SHI onto two target types: (1) a force measurement transducer (FMT)

* Fellow, Professor

Copyright © 1999 by the American Institute of Aeronautics and Astronautics Inc. All rights reserved.

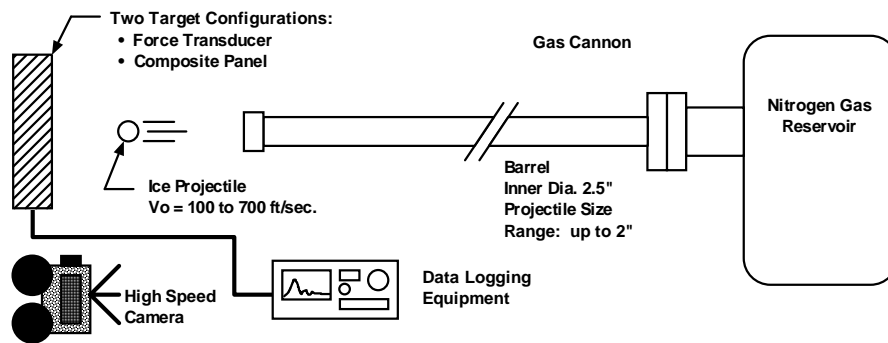


Figure 1. Nitrogen Gas Cannon Experimental Setup at Pratt & Whitney East Hartford

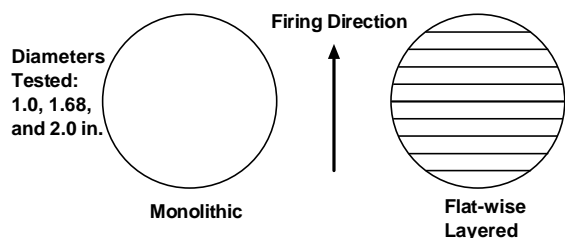


Figure 2. Simulated Hail Ice (SHI) Construction; Monolithic or Layered

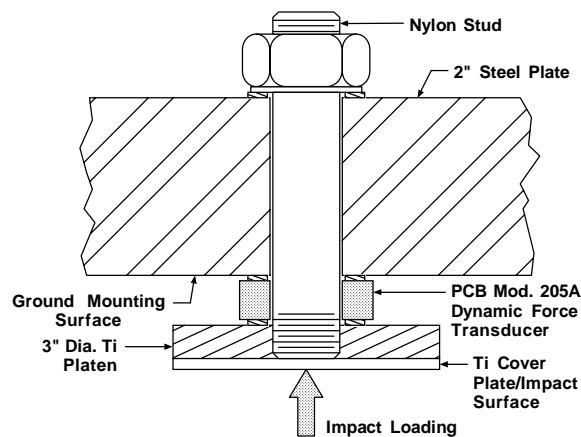


Figure 3. Force Measurement Transducer (FMT) Target

system, and (2) composite panel targets. The FMT, shown in Figure 3, consists of a piezo-electric force ring mounted between a titanium platen and a thick steel plate. The FMT measured the dynamic force history of an ice sphere impacting this instrumented target to assist in understand the behavior of ice during high velocity impacts. High speed film photography was used to observe the kinematic behavior of the ice during the impact event. Figure 4 shows two still images from high speed filming of ice impacting the FMT at 241 ft/sec. As seen in the photos, the ice sphere

locally crushes immediately upon contact with the FMT face, and proceeds to fail locally throughout the impact event. Note how the blue dyed sphere whitens as the event proceeds. This is evidence of micro-cracking throughout the sphere. The same local crushing behavior of ice spheres impacting at high velocity was also observed by Singh, DeWitt and Britton⁸.

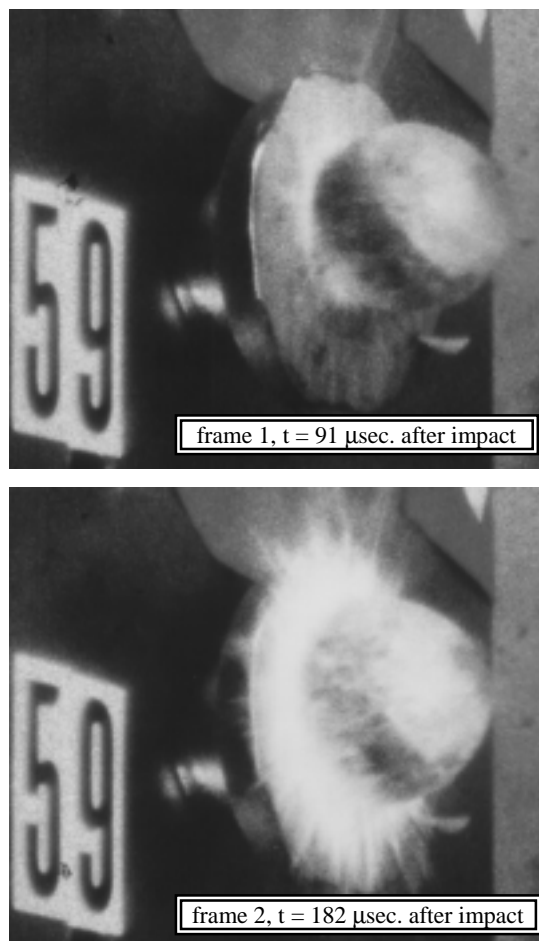


Figure 4. Still Images from High Speed Film of Test 59; 1.68 in. Diameter Layered SHI at 241 ft/sec.

As shown in Figure 5, the composite panel targets were held firmly by an aluminum picture frame fixture. All composite panels were AS4/8552 and AS4/977 fabric plates, in eight and five harness-satin weave styles, respectively, and in $\pi/4$ quasi-isotropic type layups. SHI projectiles were directed at the center of the panels, at normal and various impingement angles.

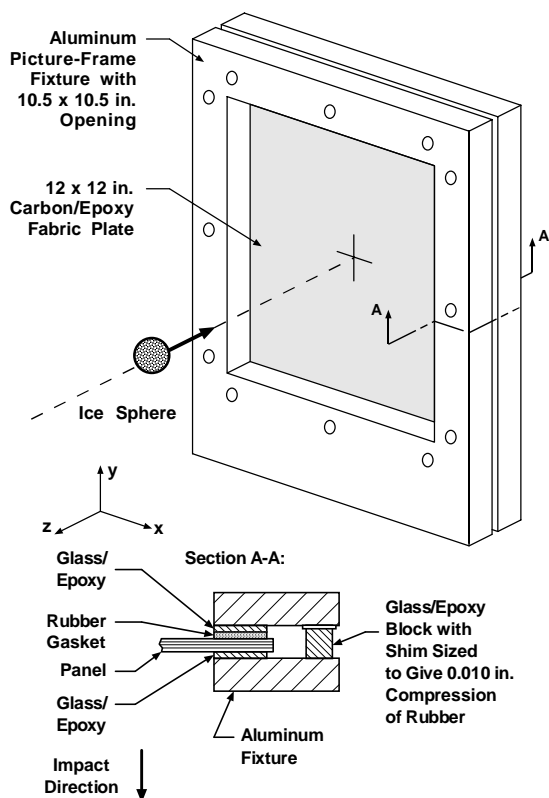


Figure 5. Composite Panel Target and Fixture Cross Sectional Detail

A series of experiments involving normal impacts of instrumented composite panels were conducted to carefully measure the panel's elastic response in order to understand the behavior of such a target when impacted by SHI. Impact experiments were also conducted to determine the multiple damage modes exhibited by the composite panels under ice impact loading. Shown in Figure 6, a progression of failure modes was observed for the composite panels as the impact threat increased. It is important to observe in Figure 6 that the severity of damage does not always increase with threat. A more threatening (i.e. higher velocity) impact could result in a damage mode, Type II for example, which is potentially less detrimental to structural performance than a failure mode caused by an impact of lower threat (i.e. lower velocity), Type I for example. Such a study of failure mode progression over a range of impact velocities is important since structural validation tests are often performed using only a single velocity based on the maximum perceived threat. This approach, often used in industry, can potentially miss some failure modes that are excited by slightly lower velocity impacts which can result in a damage mode more severe than that produced by tests of higher velocity. It should furthermore be pointed out that glancing impacts have been found to act as normal impacts with an effective velocity equal to the normal component of the projectile's true velocity^{11,12}. This reinforces the need to perform impact tests over a range of velocities to capture all failure modes, particularly since most in-flight impacts shall be of a glancing nature.

Finite Element Models

The elastic response of a composite panel impacted by a spherical ice projectile at high velocity

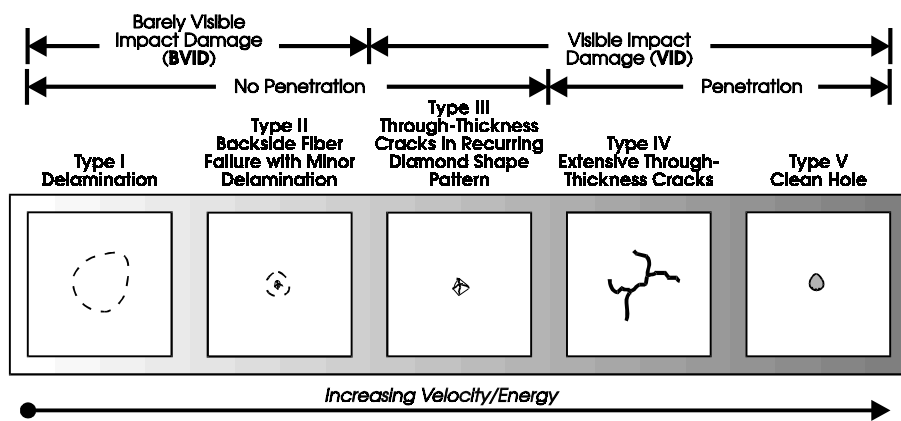


Figure 6. Failure Modes Observed Experimentally for High Velocity Ice Impacts

was simulated using the explicit finite element code *DYNA3D*¹³. In preparation for this numerical simulation, significant effort was first put into developing a suitable model for the ice projectile itself. To accomplish this, the FMT was carefully modeled using the quarter-symmetric mesh shown in Figure 7.

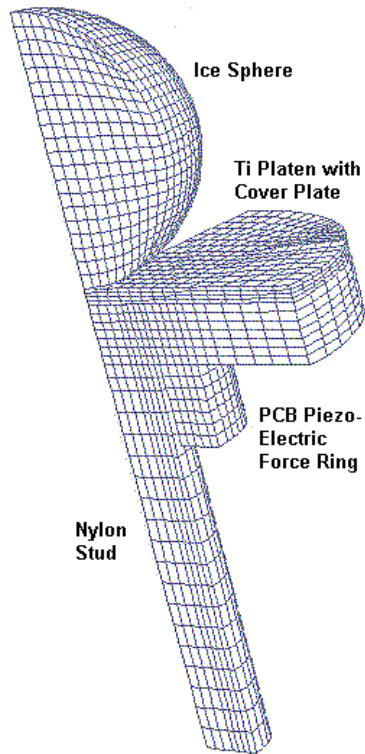


Figure 7. *DYNA3D* Quarter Model Mesh of Ice Sphere Impacting FMT

The model includes all components of the system except for the thick steel plate and the nut at the end of the nylon stud (see Figure 3). At the piezoelectric ring to steel plate interface, non-reflecting and appropriately fixed boundary conditions were specified. The non-reflecting boundary condition did not permit the reflection of stress waves when they reached this boundary. Of primary interest is the material properties used in modeling the ice sphere. Table 1 summarizes the basic material inputs used in the *DYNA3D Material Type 13 Elastic-Plastic with Failure* material model.

Properties such as shear modulus and bulk modulus were taken from the literature¹⁴⁻¹⁶. Values for hardening modulus, plastic failure strain, and failure pressure (negative value denotes tensile hydrostatic stress) were parametrically determined by comparing the numerical simulation results with the experimental data. Finally, the density was a direct measurement of the tested SHI weight divided by the spherical volume. Density was recorded for each experiment and a mean

value was used in the numerical simulations. The behavior of this material model is such that when the plastic failure strain is reached, all shear stress components are relaxed to zero. Furthermore, when the failure pressure is reached, the material is only allowed to carry hydrostatic compressive stress, thus behaving like a fluid. It should be noted that this is a simplified material model representation of such a complex material as ice. Researchers show ice to be quite complicated as it exhibits a nonlinear pressure-volume^{16,17} relationship as well as failure strength dependency on strain-rate^{9,18} and confining pressure¹⁹. In the numerical analyses, the use of the *DYNA3D Type 13 Elastic-Plastic with Failure* material model results in material behavior which has a linear pressure-volume relationship and does not exhibit any dependency of ice failure strength on strain rate and pressure.

Property	Value
Density	0.0305 lb/in ³
Elastic Shear Modulus	0.502 x 10 ⁶ psi
Yield Strength	1.5 x 10 ³ psi
Hardening Modulus	1.0 x 10 ⁶ psi
Bulk Modulus	1.305 x 10 ⁶ psi
Plastic Failure Strain	0.35 %
Tensile Failure Pressure	- 580 psi

Table 1. Ice Material Input for *DYNA3D Material Type 13 Elastic-Plastic with Failure* Model

Figure 8 shows images from a sequence of *DYNA3D* model results simulating the impact of 1.68 in. diameter SHI onto the FMT at 241 ft/sec. Comparing Figure 8 with 4, one can observe that the

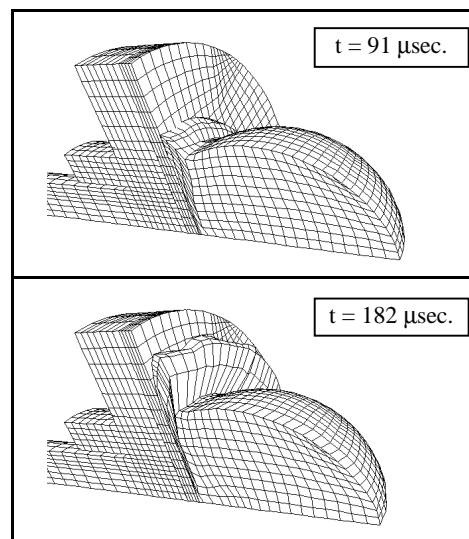
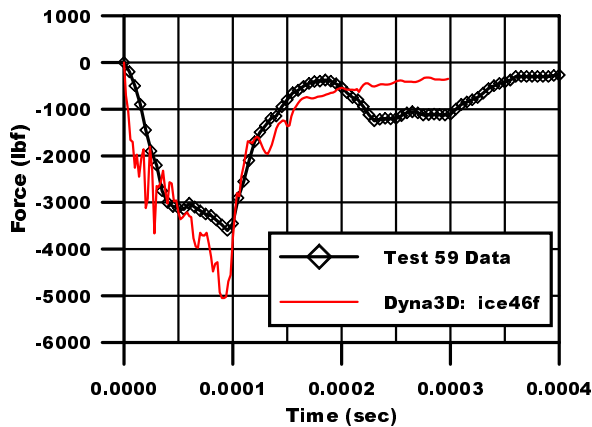


Figure 8. *DYNA3D* Simulation of Test 59; 1.68 in. Diameter Layered SHI at 241 ft/sec.

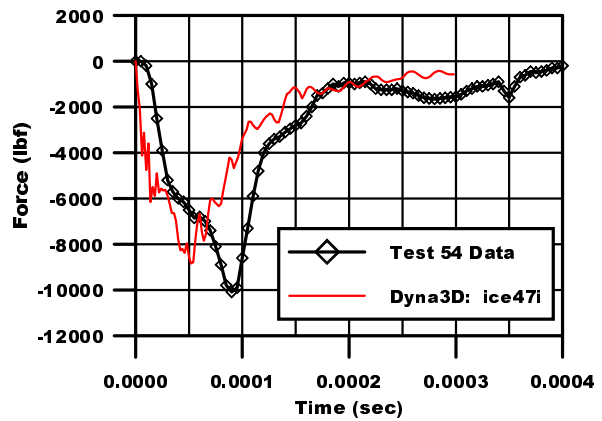
simulation captures the kinematic behavior of the ice impact experiments. Failed material flowing outwards from the impact face can be observed in the *DYNA3D* simulation. Figure 9 shows the numerically predicted force history compared with data from four different SHI impact on FMT tests. As seen in Figure 9, the peak forces and general force pulse shapes were predicted by *DYNA3D* reasonably well in each case. The major discrepancy lies in the numerically predicted time to peak force occurring before the experimentally measured time to peak. A total of five different velocity impact simulations were run with *DYNA3D*. These are summarized in Figure 10 in the form of numerically predicted peak force versus projectile kinetic energy. Also in the figure are plotted data for all tests involving SHI (both monolithic and layered, all three diameters) impacting the FMT. The relationship between measured peak force and projectile kinetic energy was found to be linear regardless of ice size for impacts of a high velocity nature (i.e. similar ice failure attributes). In the figure, it is clear that the *DYNA3D*

predictions follow the trend experimentally measured for monolithic SHI. This is an expected result as the *DYNA3D* model does not account for layered ice construction and is therefore a model of the monolithic SHI. Note however that the behavior of the two types of SHI lie within the experimental scatter of each other up to an impact energy of 300 ft-lbf. Thus the numerical model is an adequate representation for both SHI types within this range.

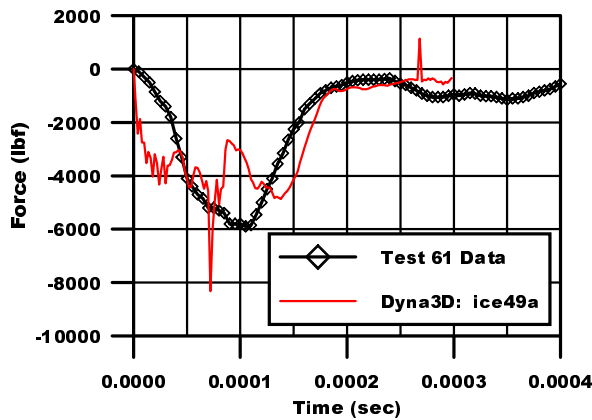
Once a reliable model for ice had been developed, the task of predicting the dynamic response of a composite panel impacted by high velocity SHI was undertaken. A test previously conducted¹¹ was chosen to be correlated with a numerical simulation using *DYNA3D*. This experiment, Test 137, involved the normal impact of 1.68 in. diameter layered SHI at a velocity of 240 ft/sec. onto a 0.096 in. thick composite panel. The panel was constructed from AS4/8552 eight harness satin fabric, having [0/45/90/-45]_S lay-up. In this test, the SHI velocity was purposely selected such that no damage was incurred by the composite panel.



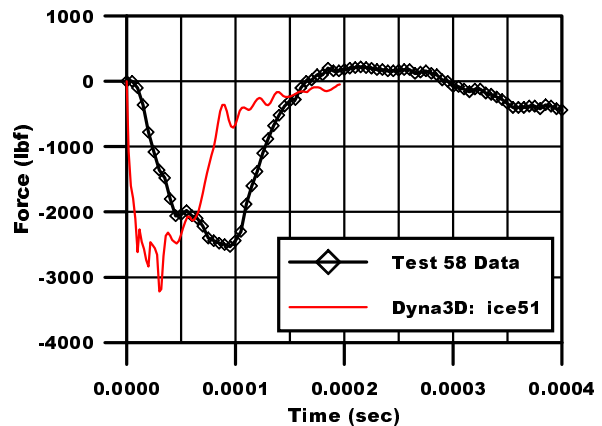
(a) Test 59: 1.68" Layered SHI at 241 ft/sec.



(b) Test 54: 1.68" Layered SHI at 414 ft/sec.



(c) Test 61: 1.68" Monolithic SHI at 313 ft/sec.



(d) Test 58: 1.0" Layered SHI at 456 ft/sec.

Figure 9. *DYNA3D* Force History Predictions of SHI Impacting FMT

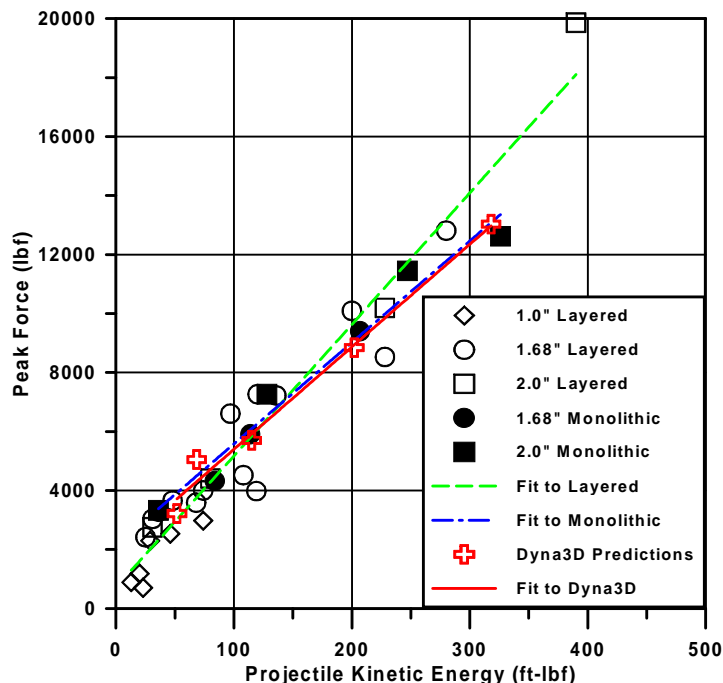


Figure 10. Summary of Peak Forces for all SHI on FMT Tests Along With *DYNA3D* Results

The plate was instrumented with four strain gauges, the locations for which are shown in Figure 11. In addition to the strain gauge instrumentation, high speed film photography was taken of the impact event from which the panel center deflection time history was measured.

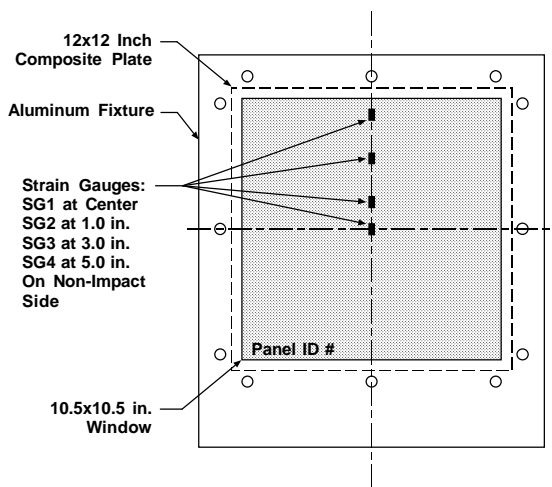


Figure 11. Composite Panel Strain Gauge Locations

Figure 12 shows the *DYNA3D* quarter model mesh for this problem. Note that to accurately represent the experimental test conditions, the exact panel boundary conditions, including the glass/epoxy and silicone rubber blocks, needed to be modeled. The entire model was created from 8-noded solid elements. A total of seven layers of solid elements, one for each

ply grouping, was used to model the panel. Each layer was given the orthotropic elastic properties listed in Table 2, with the ply angle specified on a layer-to-layer basis. Solid elements were chosen over more computationally efficient shell elements due to the inherent limitations of shell elements when predicting out-of-plane stress components. The importance for predicting out-of-plane stress components is a consideration for future plans of predicting impact damage, particularly delamination and out-of-plane stress dominated failure modes.

$E_{11} = 10.4 \text{ Msi}$	$E_{22} = 10.09 \text{ Msi}$	$E_{33} = 1.0 \text{ Msi}$
$G_{12} = 0.75 \text{ Msi}$	$G_{23} = 0.75 \text{ Msi}$	$G_{13} = 0.75 \text{ Msi}$
$\nu_{21} = 0.038$	$\nu_{31} = 0.029$	$\nu_{32} = 0.030$

Table 2. AS4/8552 Eight Harness Satin Fabric Properties Used in *DYNA3D* Modeling

The ice sphere shown in Figure 12 was imported from the same models previously developed for SHI impacting the FMT. A frictional sliding interface was specified between the panel and the sphere, which was given a velocity initial condition of 240 ft/sec. Figure 13 shows the predicted panel center deflection along with the experimentally measured center deflection history for Test 137. Also shown in the figure is the contact force history at the sphere to panel interface. The time axes of these two plots are aligned to assist in understanding the kinematics of the

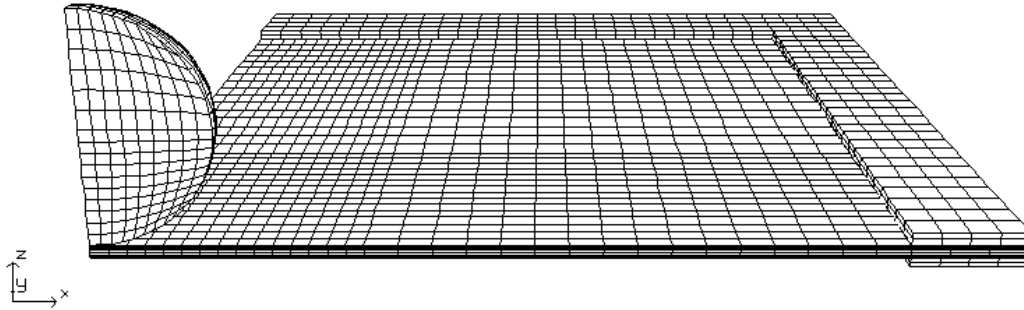


Figure 12. *DYN3D* Mesh of 1.68 in. Diameter SHI Impacting Composite Panel

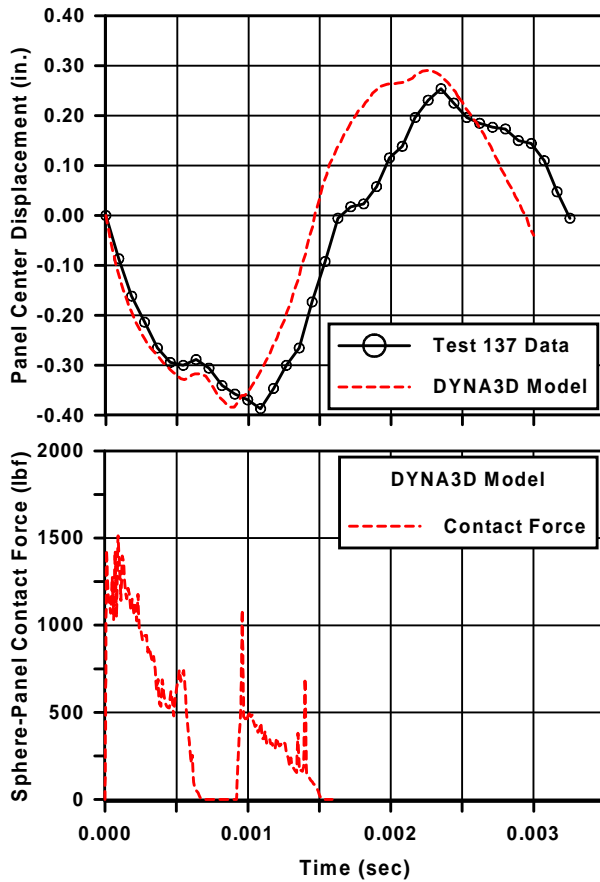


Figure 13. *DYN3D* Simulation: 1.68 in. Diameter Layered SHI Impacting Fabric Panel at 240 ft/sec.

event. The SHI loads up the panel which quickly reaches a displacement of 0.32 in. At this time a slight rebound of the panel causes a momentary loss of sphere to panel contact between the times 0.7 to 0.9 msec. The panel then reaches its maximum displacement of 0.38 in., and in fully rebounding towards zero displacement, pushes the SHI mass backwards with a nontrivial amount of force, as seen by the second force pulse. Finally, well before the panel nears its second displacement peak, the ice mass is completely ejected

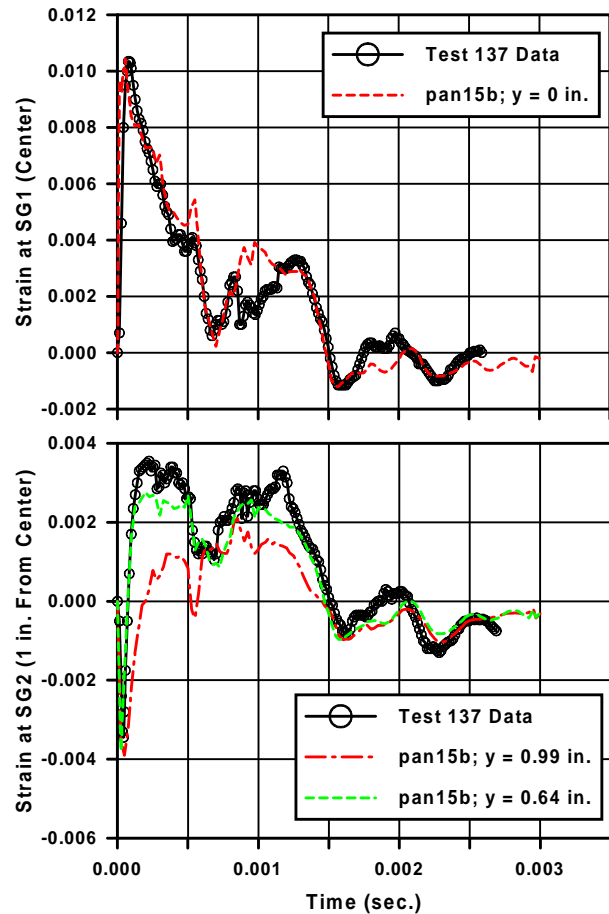


Figure 14. *DYN3D* Predicted Strain History and Test 137 Data

away at a time of 1.5 msec. At this time the analysis is stopped with a restart file written, the elements representing the ice are removed, and the revised model containing only the elements associated with the target is then restarted and allowed to run until completion.

Figure 14 shows the predicted panel strain histories at locations SG1 (backside, center) and SG2 (backside, 1.0 in. from center). As seen in the figure, the finite element model predicts the center strain gauge SG1 history quite well. The peak strain, time to peak,

and general overall trend matches the experimentally measured strain history closely. At location SG2, the *DYNA3D* prediction does not match the experimental strain as closely when the finite element model results are taken at 0.99 in. from the panel center. However, when finite element model results are taken at a distance of 0.64 in. from the panel center, the results agree with the experimental measurement very well. One simple explanation for this is that in the experiments, the ice sphere missed the intended impact location by 0.36 in. (1.0 minus 0.64 in.). However, if this were the case, then finite element results taken at 0.36 in. from the panel center should match up with the experimental measurements of SG1. This unfortunately was not so.

Figures 15 to 18 show contour plots of shear stress τ_{xz} through the cross-section of the panel at times of $t = 6, 12, 18,$ and $25 \mu\text{sec}$. A dark triangle marks the location of maximum positive shear stress. This stress develops at the boundary of the contact patch which the SHI makes as it crushes onto the panel. The shear stress is a maximum soon after the impact event occurs (at $12 \mu\text{sec}$), and decreases as the contact patch grows. Another observation to note is the through-thickness location of the maximum shear stress. It starts near the center, and as time goes on moves closer to the backside of the panel, away from the impact face.

Conclusions

The impact of a high velocity ice sphere onto a carbon/epoxy composite panel was successfully simulated using the explicit finite element code *DYNA3D*. In support of this panel impact simulation, a suitable ice projectile material model was first developed by conducting simulations of simulated hail ice (SHI) impacting the instrumented force measurement transducer (FMT) system. From these initial FMT models, the following conclusions can be drawn. The kinematic behavior of these numerical models matches the experimentally observed behavior. The peak forces predicted by the *DYNA3D* simulations match the experimental data for SHI of monolithic construction. Over the studied range of velocity, 100 to 500 ft/sec., the ice material can successfully be modeled using the simple *DYNA3D Material Type 13 Elastic-Plastic with Failure* material model, without accounting for complex pressure-volumetric behavior and failure strength sensitivity to strain rate and pressure. This model, once developed, can readily be applied in *DYNA3D* to impact onto any structure.

The results of the panel elastic response prediction matched with the experimentally measured response. The center deflection history matched the

test data well, particularly during the first peak of the oscillation. Since the panel and the ice sphere are no longer in contact during the second oscillation peak, one can argue that any damage formation for this class of impacts shall occur at some time during the first peak. Furthermore, the strain gauge test data at the center of the panel and at 1.0 in. distance away both go to zero after a time of 1.5 ms. This coincides with the time when the contact force between the ice and the panel was predicted to go to zero due to the ice being ejected away from the panel. At this time, the panel center also begins its second oscillation peak. Another observation to note is that the peak force during contact of the ice with the panel occurs almost immediately, as well as peak strains. This fact together with the contact patch being initially small means that very high pressures are being applied to the panel face. Finally observe that the panel peak displacement does not coincide with the time of peak contact force. In fact the panel center reaches maximum displacement at a time when the contact force is momentarily zero. This observation highlights the fact that these impacts are high velocity and quite dynamic in nature, and simple quasi-static based analyses, common and valid when dealing with low velocity impacts, can not be applied to problems of this nature. The predicted strain at the center of the panel matches the test data quite well in both peak magnitudes and general shape. Conversely, the strain prediction by the finite element model at 1.0 in. distance from the center does not match the test data of a strain gauge at that location. The strain prediction at a distance of 0.64 in. from the center however does match the test data quite well. An immediate simple explanation is that in the experiments, the ice sphere impact point was off target and a data collection location correction needs be made to account for this. Unfortunately, applying such a simple correction does not accomplish as good a fit to the strain data for the panel center as when model results were taken at the uncorrected panel center. Another explanation is in the ice sphere material model itself being stiffer than actuality. Observing the predicted force measurements on the FMT, Figure 9, and the panel center deflection history, Figure 13, the predicted initial response of these systems occurs at a faster time scale than the test data. In choosing to model the ice sphere using the simple *DYNA3D Elastic-Plastic with Failure* material model, it is conceivable that ignoring the actual complex behavior of the ice material itself is resulting in an overly stiff ice material response. Despite this concern, the simple material model does capture the primary features of ice impact behavior as evidenced by the results reported herein.

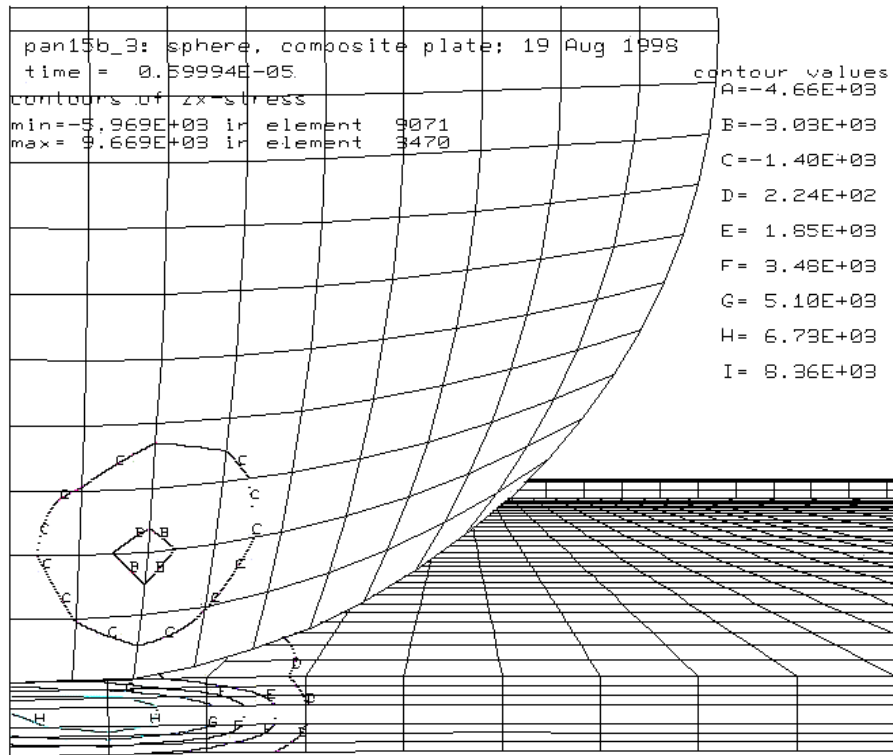


Figure 15. DYNA3D Panel Impact Simulation; $t = 6 \mu\text{sec.}$, Maximum $\tau_{xz} = 9.67 \text{ ksi}$

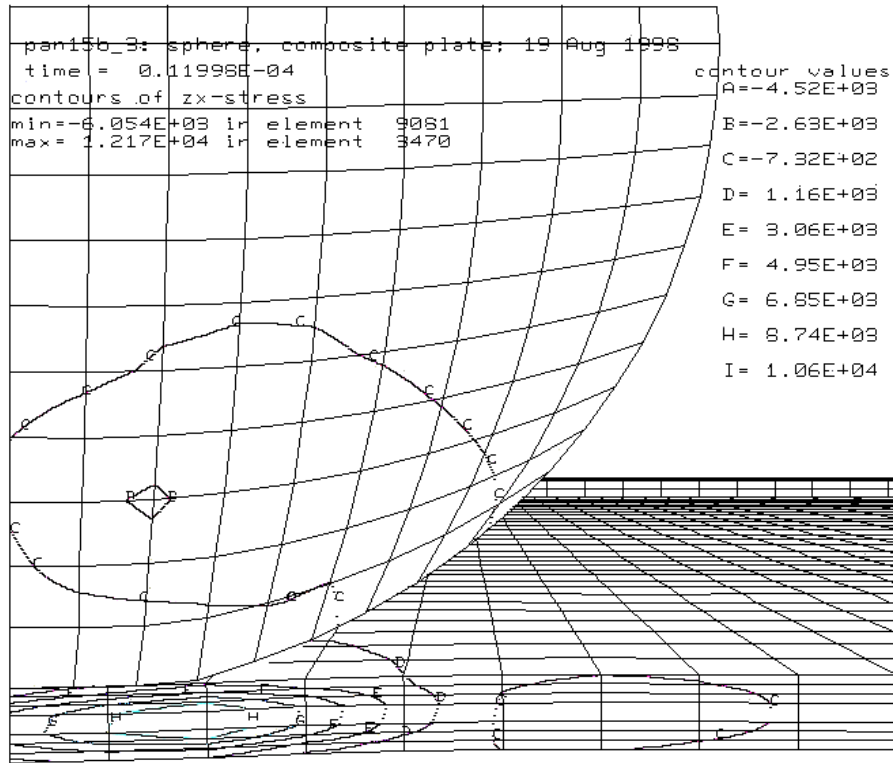


Figure 16. DYNA3D Panel Impact Simulation; $t = 12 \mu\text{sec.}$, Maximum $\tau_{xz} = 12.2 \text{ ksi}$

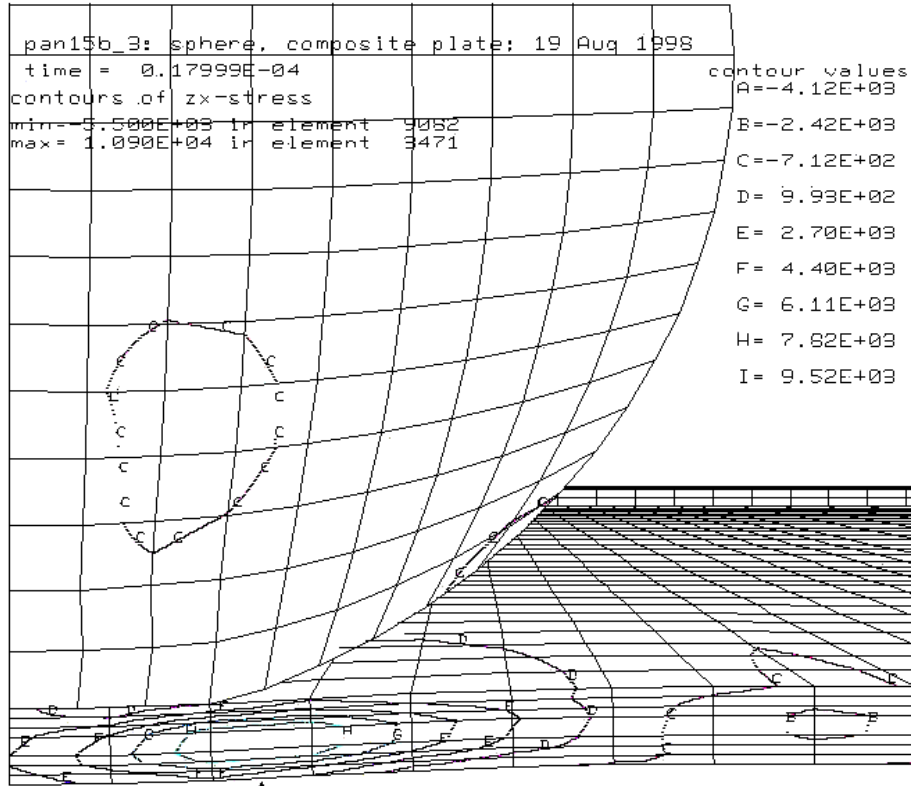


Figure 17. DYN3D Panel Impact Simulation; $t = 18 \mu\text{sec.}$, Maximum $\tau_{xz} = 10.9 \text{ ksi}$

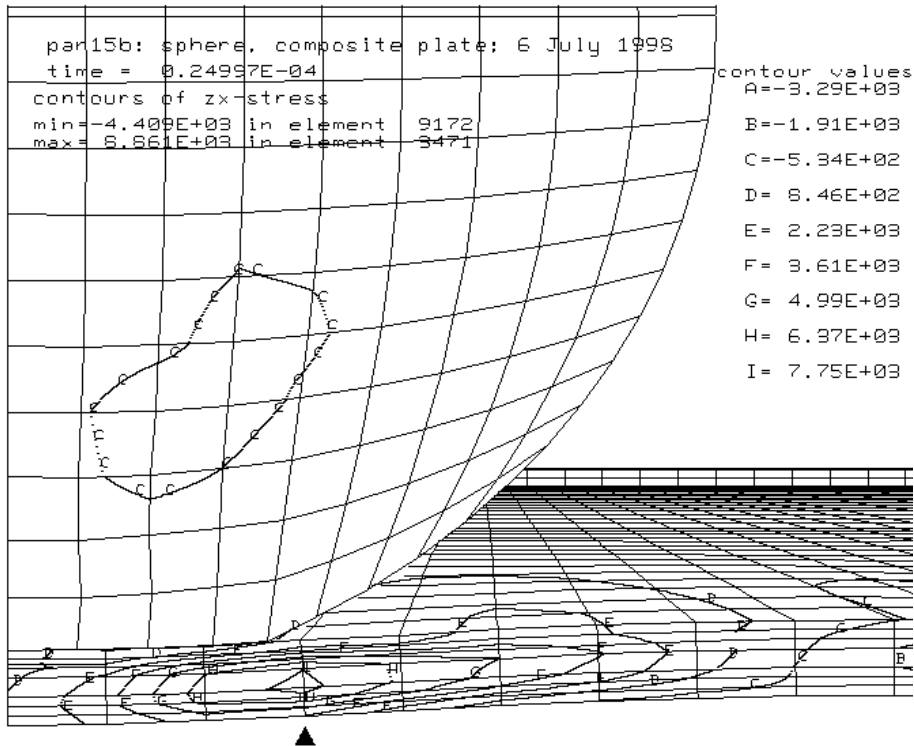


Figure 18. DYN3D Panel Impact Simulation; $t = 25 \mu\text{sec.}$, Maximum $\tau_{xz} = 8.86 \text{ ksi}$

Acknowledgements

This work was supported through the Pratt & Whitney led and DARPA funded Affordable Composites for Propulsion (ACP) program. Special thanks to Rajiv Naik, Gary Griesheim, Craig Musson, Doug Welch, and Tom Vasko of Pratt & Whitney, William Adler of General Research Corporation International, and Chuck Charman of the San Diego Supercomputer Center. All DYN3D computations were run on the National Partnership for Advanced Computational Infrastructure (NPACI) San Diego Supercomputer Center (SDSC) Cray T90.

References

1. Jackson, W. C., and Poe, C. C. Jr., "The Use of Impact Force as a Scale Parameter for the Impact Response of Composite Laminates," NASA Technical Memorandum 104189, AVSCOM Technical Report 92-B-001, January 1992.
2. Greszczuk, L. B., "Damage In Composite Materials Due to Low Velocity Impact," *Impact Dynamics*, edited by L. A. Zukas *et al.*, John Wiley and Sons, New York, 1982, pp. 55-94.
3. Shivakumar, K. N., Elber, W., and Illg, W., "Prediction of Impact Force and Duration Due to Low-Velocity Impact on Circular Composite Laminates," *Transactions of the ASME*, September 1985, Vol. 52, pp. 674-680.
4. Sjöblom, P., "Simple Design Approach Against Low-Velocity Impact Damage," *Proceedings of the 32nd International SAMPE Symposium*, April 6-9, 1987, pp. 529-593.
5. Joshi, S. P. & Sun, C. T., Impact induced fracture in a quasi-isotropic laminate. *Journal of Composites Technology and Research*, Vol. 9, 1987 40-46.
6. Joshi, S. P. & Sun, C. T., Impact induced fracture in a laminated composite. *Journal of Composite Materials*, Vol. 19, 1985 51-66.
7. Guynn, E. G. & O'Brien, T. K., The influence of lay-up and thickness on composite impact damage and compression strength. *A Collection of Technical Papers: AIAA/ASME/ASCE/AHS 26th Structures Conference, April 15-17, Orlando, Florida, 1985*, 187-196.
8. Singh, S., DeWitt, K. J., and Britton, R. K., "Measurements of the Impact Forces of Shed Ice Striking a Surface," *AIAA 32nd Aerospace Sciences Meeting and Exhibit*, Paper No. AIAA-94-07-0713, Reno, NV, January 10-13, 1993.
9. Jones, S. J., "High Strain-Rate Compression Tests on Ice," *Journal of Physical Chemistry B*, Vol. 101, No. 32, 1997, pp. 6099-6101.
10. Schulson, E. M., "The Brittle Failure of Ice Under Compression," *Journal of Physical Chemistry B*, Vol. 101, No. 32, 1997, pp. 6254-6258.
11. Kim, H., and Welch, D. A., "Investigation of Hail Ice Impact on Composite Structures," Pratt & Whitney Technical Report, EII No. 95-200-0035-B, June 1, 1995.
12. Ghaffari, S., Tan, T.-M., and Awerbuck, J., "An Experimental and Analytical Investigation on the Oblique Impact of Graphite/Epoxy Laminates," *Proceedings of the 22nd International SAMPE Technical Conference*, November 6-8, 1990, pp. 494-508.
13. Whirley, R. G., and Engelmann, B. E., "DYN3D A Nonlinear, Explicit, Three-Dimensional Finite Element Code For Solid and Structural Mechanics – User Manual," Lawrence Livermore National Laboratory, UCRL-MA-107254 Rev. 1, November 1993.
14. Batto, R. A. and Schulson, E. M., "On the Ductile-to-Brittle Transition in Ice Under Compression," *Acta Metallurgica et Materialia*, Vol. 41, No. 7, 1993, pp. 2219-2225.
15. Schulson, E. M., "The Brittle Compressive Fracture of Ice," *Acta Metallurgica et Materialia*, Vol. 38, No. 10, 1990, pp. 1963-1976.
16. Mellor, M., "Mechanical Properties of Polycrystalline Ice," *Physics and Mechanics of Ice*, edited by Per Tryde, IUTAM Symposium, Copenhagen, 1979, Springer-Verlag, New York, 1980, pp. 217-245.
17. Schroeder, R. C. and McMaster, W. H., "Shock-Compression Freezing and Melting of Water and Ice," *Journal of Applied Physics*, Vol. 44, No. 6, June 1973, pp. 2591-2594.
18. Mellor, M. and Cole, D. M., "Deformation and Failure of Ice Under Constant Stress or Constant Strain-Rate," *Cold Regions Science and Technology*, Vol. 5, 1982, pp. 201-219.
19. Nadreau, J. P., Mawwar, A. M., and Wang, Y. S., "Triaxial Testing of Freshwater Ice at Low Confining Pressures," *Proceedings of the Seventh International Conference on Offshore Mechanics and Arctic Engineering*, Houston, TX, February 7-12, 1988, pp. 117-124.